Supporting Information

The Structural Basis of the Green-Blue Color Switching in Proteorhodopsin as determined by NMR Spectroscopy

Jiafei Mao[1], Nhu-Nguyen Do[1], Frank Scholz[2], Lenica Reggie[1], Michaela Mehler[1], Andrea Lakatos[1], Yean-Sin Ong[1], Sandra J. Ullrich[1], Lynda J. Brown[3], Richard C. D. Brown[3], Johanna Becker-Baldus[1], Josef Wachtveitl[2], and Clemens Glaubitz[1]*

(1) Institute of Biophysical Chemistry & Centre for Biomolecular Magnetic Resonance, Goethe-University Frankfurt, Germany

(2) Institute of Physical and Theoretical Chemistry

(3) Department of Chemistry, University of Southampton

(*) Corresponding author.

Email: glaubitz@em.uni-frankfurt.de
Institute of Biophysical Chemistry
Goethe University Frankfurt
Max-von-Laue-Str. 9
60438 Frankfurt am Main
Germany
Tel.: +49-69-798-29927
Fax.: +49-69-798-29929

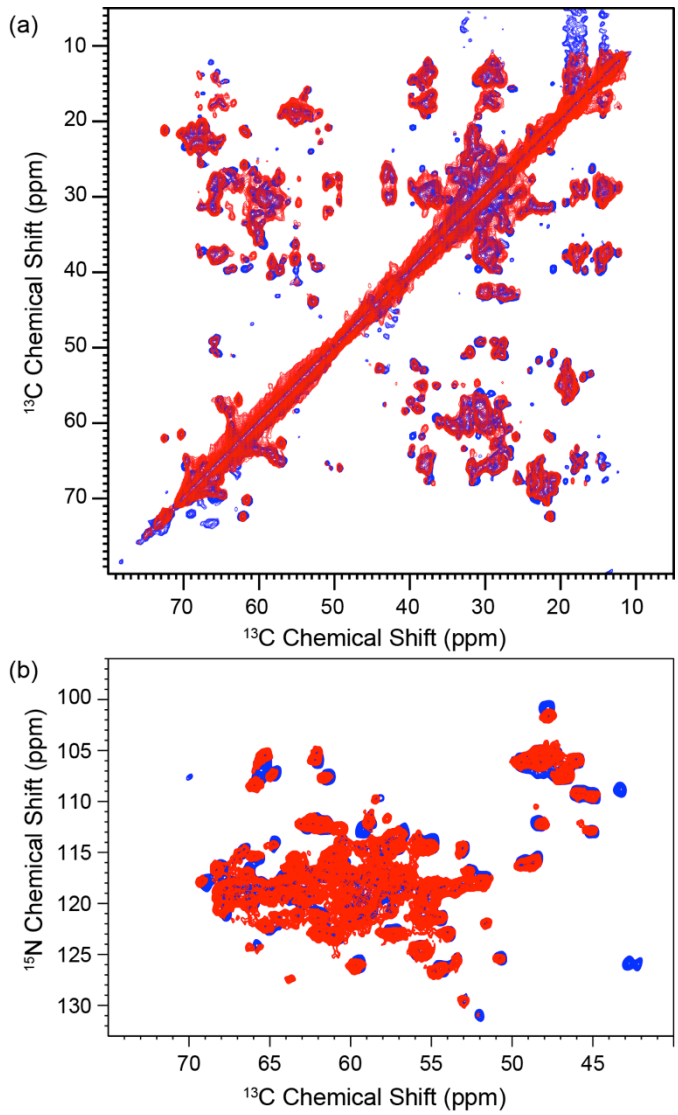

Fig. S1: (a) ^{13}C-^{13}C DARR (20 ms mixing time) and **(b)** ^{15}N-^{13}C NCA spectra of GPR (blue) and GPR_{L105Q} (red) show similar overall spectral patterns between both constructs. For experimental details see Materials and Methods section.

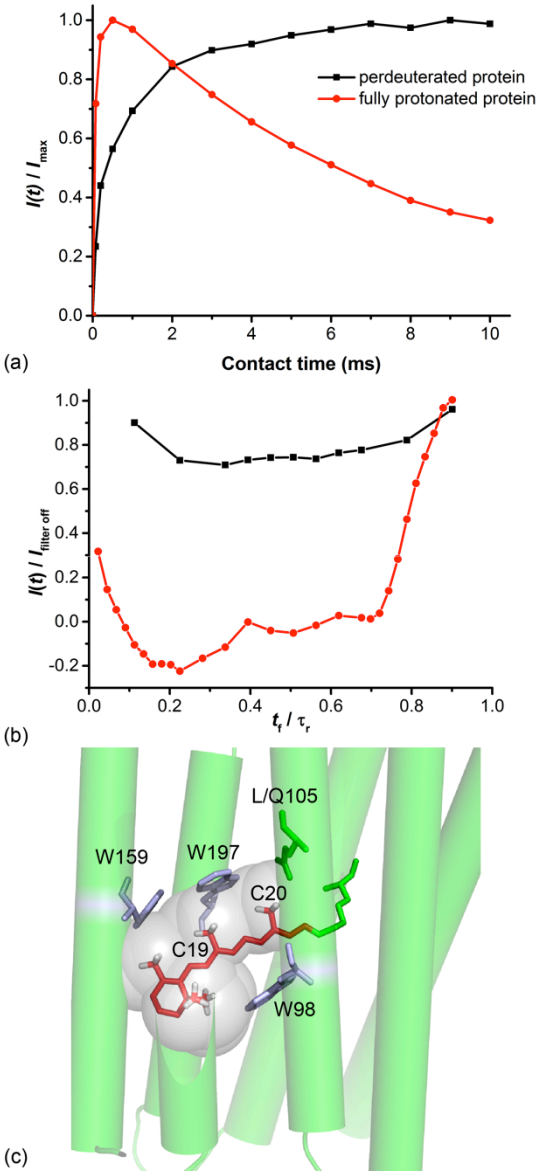

Fig. S2: (a) Calibration of cross polarization build-up and **(b)** MELODI [1] dephasing kinetics of fully protonated (black) and perdeuterated GPR (red). The protonated samples show steep increase followed by a rapid decay of their cross polarization intensity. In contrast, deuteration leads to a much slower build-up, which is due to the highly diluted proton spin reservoir. In **(b)** it is shown that the MELODI dephasing scheme could efficiently remove the signals from ^{13}C in close contact with ^{1}H. This is generally the case in protonated samples but also applied to carbons directly bound to residual protons in perdeuterated samples. The asymmetry of the dephasing curve may be due to the finite pulses used in the scheme. **(c)** The application of ^{1}H-^{13}C MELODI-HETCOR to U-^{13}C, ^{2}H-GPR and GPR_{L105Q} in complex with fully protonated retinal cofactor enabled to probe long distance contacts especially between protons at C19/C20 and carbons in W197 (see main text and Fig. 2d). The model is based on the BPR X-ray structure 4JQ6.[2] For experimental details see Materials and Methods section.

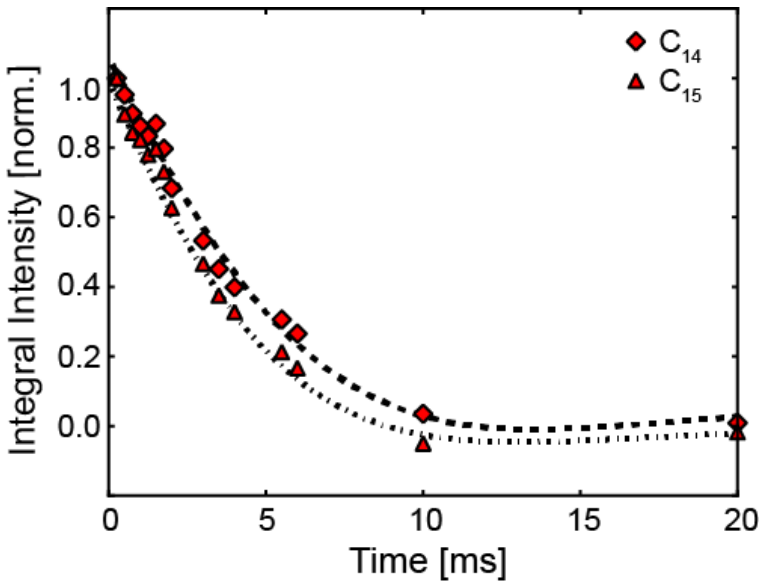

Fig. S3: Spin-echo experiments on 14,15-^{13}C-all-*trans*-retinal bound to GPR under DNP conditions. Data points were recorded with different number of scans (256 - 4096) depending on S/N and integral intensities were calibrated accordingly. The curves were fitted to the function I(t)=Exp(-t/T_2)*Cos(π*J*t) using a ^{13}C-^{13}C J-coupling value of 55 Hz for a trans-like conformation.[3,4] The fitted T2' is 5.7 and 4.7 ms, corresponding to line width of 56 Hz and 68 Hz, for C14 and C15, respectively. For experimental details see Materials and Methods section.

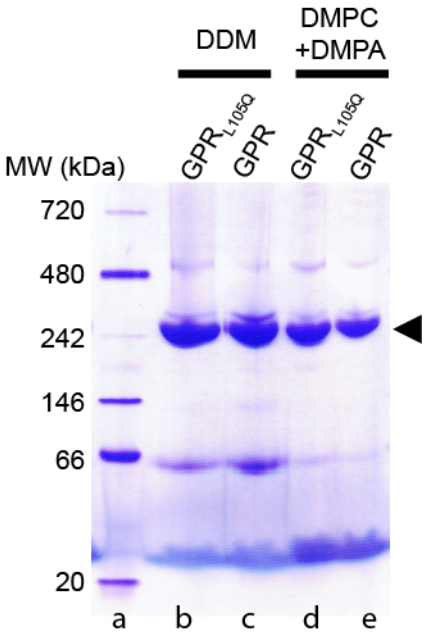

Fig. S4: Blue-Native PAGE analysis [5] shows the same dominating oligomeric state of GPR and GPR_{L105Q} in both detergent and lipid environment. **Lane a:** molecular weight marker; **Lane b-c:** GPR_{L105Q} and GPR in DDM (0.3 %); **Lane d-e:** GPR_{L105Q} and GPR reconstituted in DMPC/DMPA liposome as used for MAS-NMR experiments in this work. The black arrow shows that the main bands in all four samples migrate almost equally on the gel. This clearly indicates that GPR and GPR_{L105Q} are in the same oligomeric state in both DDM micelle and DMPC/DMPA liposomes. It is known from previous studies that GPR forms pentamers in DDM micelles and membranes and hexamers in 2D-crystal preparations.[6,7] Blue-native PAGE analysis was performed using NativePAGE Novex® Bis-Tris gel system following the standard protocol provided by the company.

Table S1. ^{13}C and ^{15}N chemical shifts (ppm) of GPR_{L105Q} assigned on ^{13}C-^{13}C and ^{15}N-^{13}C MAS-NMR spectra. The ^{13}C chemical shifts are referenced via adamantane to DSS. ^{15}N chemical shifts are referenced indirectly via the $^{13}C/^{15}N$ gyromagnetic ratios to and liquid NH_3 at 0 ppm. Ambiguous assignments are highlighted in red. The chemical shift differences ($\delta(GPR_{L105Q}) - \delta(GPR)$) are given in parentheses. The average chemical shift change is 0.4 ppm. A small set of 10 residues (T69, E85, T101, I112, A115, A116, I145, A185, T188, I194) has been found to show unambiguous ^{13}C chemical shift changes on side chain and/or backbone larger than the average chemical shift differences.

Sequential Number	Residue Type	N	C'	Cα	Cβ	Cγ	Cγ1	Cγ2	Cδ	Cδ1	Cδ2	Cε
29	Thr	107.1 (0.0)		64.8 (0.1)	69.7 (0.1)			22.4 (0.2)				
30	Gly	109.0 (- 0.1)	174.8 (0.2)	45.8 (- 0.1)								
37	Thr	117.8 (0.2)	175.8 (0.1)	69.3 (0.1)	68.1 (- 0.4)			22.9 (0.0)				
38	Ala	121.1 (0.2)			18.5 (0.0)							
39	Ala	118.6 (- 0.1)	180.5 (0.0)	55.2 (0.1)	19.9 (0.0)							
43	Ser	112.0 (0.1)	173.5 (0.3)	62.6 (0.2)	62.3 (0.2)							
44	Thr	118.6 (0.2)	173.6 (- 1.0)	67.5 (- 0.2)	68.9 (0.0)			21.0 (0.1)				
63	Thr			62.8 (0.1)	66.8 (- 0.3)							
69	Thr	105.3 (- 0.8)	177.5 (0.2)	65.2 (- 0.3)	66.9 (-0.3)			23.2 (0.2)				
70	Gly	116.0 (0.4)	175.9 (0.3)	48.6 (0.3)								
71	Ile	124.3 (0.1)	177.3 (- 0.3)	65.8 (0.0)	38.3 (0.3)			19.1 (0.2)		14.4 (0.2)		
72	Ala	120.3 (0.0)	179.4 (0.3)	55.4 (0.0)	19.8 (0.2)							
85	Glu			58.3 (- 0.5)	29.7 (- 0.9)	36.4 (0.2)			183.9 (0.4)			
86	Thr	105.7 (- 0.2)	176.2 (0.2)	62.2 (0.1)	72.3 (0.0)			21.2 (0.1)				
87	Gly	112.7 (- 0.1)	171.2 (0.2)	45.0 (0.0)								
88	Asp	116.7 (- 0.2)	174.8 (0.0)	52.7 (0.2)	44.0 (0.1)	181.1 (0.3)						
89	Ser	112.9 (0.1)	172.1 (- 0.3)	57.2 (0.3)	65.4 (0.2)							
90	Pro		180.0 (0.2)	63.5 (0.3)	32.7 (0.2)							
91	Thr	119.6 (- 0.1)	178.3 (0.0)	66.3 (0.1)	67.5 (0.0)	22.7 (- 0.2)						
97	Asp	113.5 (- 1.1)	178.1 (- 0.4)	55.8 (- 0.1)	42.0 (- 0.3)	175.4 (0.0)						
101	Thr	108.2 (0.6)	177.1 (0.0)	65.9 (0.2)	69.0 (- 0.8)	24.0 (0.7)						
103	Pro	135.3 (0.3)		65.3 (0.0)	31.8 (0.1)				50.9 (0.0)			
107	Cys		177.5 (0.2)	63.6 (- 0.3)	26.8 (0.2)							
108	Glu	119.7 (- 1.0)		59.0 (0.1)	28.4 (0.1)							
112	Ile	114.3 (0.6)		64.7 (0.1)	37.9 (- 0.3)		26.3 (- 0.2)	18.3 (- 0.1)		15.7 (- 0.1)		
114	Ala	122.8 (- 0.1)	179.2 (0.1)	53.9 (0.0)	16.9 (0.2)							
115	Ala	118.5 (0.1)	177.6 (- 0.1)	53.4 (0.1)	15.9 (0.4)							
116	Ala	117.7 (- 0.5)		53.0 (0.0)	24.0 (0.1)							
126	Lys	116.9 (- 0.1)	178.7 (0.1)	60.6 (0.0)	34.6 (0.2)	26.6 (0.0)						42.9 (0.2)
134	Met	116.9 (- 0.4)	176.9 (0.1)	59.9 (0.2)	35.0 (0.0)	30.2 (0.0)						

138	Gly	106.0 (- 0.2)	175.3 (0.0)	49.3 (0.1)						
140	Met	115.0 (- 0.1)	179.7 (0.2)	60.9 (0.1)	34.4 (0.0)	32.5 (0.0)				
141	Gly	107.2 (- 0.2)	176.7 (0.4)	46.6 (0.1)						
142	Glu	122.9 (- 0.2)	178.3 (- 0.1)	61.0 (- 0.1)	29.2 (- 0.2)	39.4 (- 0.2)			179.7 (0.7)	
143	Ala	117.6 (0.1)		51.9 (0.0)	19.0 (0.2)					
144	Gly	105.8 (- 0.2)	174.6 (- 0.1)	45.9 (0.1)						
145	Ile	121.3 (0.3)	175.1 (0.5)	63.3 (0.1)	39.5 (0.1)		29.2 (0.2)	17.8 (0.2)		14.2 (- 0.1)
146	Met	114.5 (0.0)	173.9 (0.1)	53.1 (0.2)	37.9 (- 0.1)	32.2 (0.1)				
148	Ala	124.3 (- 0.1)	182.0 (0.0)	55.9 (0.1)	19.1 (0.2)					
150	Pro	132.2 (- 0.2)		66.3 (- 0.2)					49.0 (- 0.2)	
151	Ala			56.6 (0.0)	18.7 (0.2)					
153	Ile	118.2 (- 0.3)	177.0 (- 0.1)		37.9 (0.0)			17.3 (0.0)		
154	Ile	118.1 (0.0)	177.5 (0.0)	65.7 (0.1)	37.0 (- 0.1)			16.5 (0.1)		13.5 (0.3)
155	Gly	105.5 (0.0)	176.0 (0.1)	48.3 (0.1)						
156	Cys	119.1 (0.0)	177.4 (0.3)	64.9 (- 0.2)	27.8 (0.3)					
162	Met	116.9 (- 0.3)	177.7 (0.1)	60.9 (0.0)	33.6 (- 0.2)	32.3 (0.1)				
163	Ile	116.7 (- 0.2)	177.5 (0.2)	66.3 (- 0.1)	37.6 (0.1)		28.8 (- 0.1)	18.4 (0.3)		12.2 (0.1)
168	Ala	117.6 (0.3)		51.7 (0.1)	22.8 (0.1)					
169	Gly	109.4 (0.0)	174.7 (0.1)	45.0 (0.1)						
170	Glu	125.8 (- 0.1)	180.1 (0.4)	59.7 (0.2)	30.9 (0.3)	36.6 (0.4)				
171	Gly		174.4 (0.2)	48.0 (0.1)						
172	Lys	122.8 (0.0)	178.4 (0.4)	57.4 (- 0.1)	30.4 (0.1)	23.8 (0.3)			27.8 (0.0)	
174	Ala	121.1 (- 0.2)	180.4 (0.4)	54.5 (0.1)	19.2 (0.3)					
175	Cys	122.6 (0.0)	176.3 (0.1)	61.8 (0.0)	25.8 (0.1)					
176	Asn	114.3 (0.0)	176.0 (- 0.1)	55.1 (0.1)	38.2 (- 0.1)	175.5 (0.0)				
177	Thr	107.5 (- 0.1)	174.2 (0.3)	61.5 (0.0)	70.1 (-0.1)			21.7 (0.2)		
178	Ala	125.2 (- 0.2)	176.3 (0.1)	50.7 (0.0)	20.9 (0.1)					
179	Ser	117.3 (0.0)	173.2 (0.3)	56.9 (0.0)	62.6 (0.0)					
180	Pro	134.9 (- 0.1)	179.7 (0.4)	65.9 (- 0.2)	31.9 (0.1)	28.2 (0.2)			50.4 (0.1)	
181	Ala		180.8 (0.0)	55.2 (0.0)	18.5 (0.3)					
183	Gln	118.8 (- 0.2)	178.5 (0.0)	60.1 (0.0)	27.7 (0.1)	34.2 (0.2)			180.7 (0.0)	
185	Ala	124.5 (-0.1)	177.9 (0.3)		18.6 (0.5)					
187	Asn	117.0 (- 0.3)	176.8 (0.0)	56.7 (0.1)	38.4 (- 0.1)	175.2 (- 0.4)				
188	Thr	116.5 (- 0.5)		68.2 (0.0)				22.8 (0.1)		
189	Met		179.0 (0.2)							
190	Met	119.7 (- 0.4)		59.4 (0.0)	32.9 (0.1)	31.1 (0.0)				
194	Ile	118.1 (0.6)	174.8 (0.4)	64.1 (- 0.2)	39.6 (- 0.1)		28.2 (0.2)	16.6 (0.0)		14.6 (0.1)
196	Gly	106.2 (- 0.7)	179.0 (0.4)	48.2 (0.3)						
199	Ile			61.6	38.1					

				(- 0.5)	(0.0)					
201	Pro	135.1 (0.0)	179.7 (0.4)	65.8 (0.1)	30.5 (0.1)	27.4 (0.0)			49.3 (0.0)	
203	Gly	112.0 (- 0.1)	177.6 (0.1)	48.1 (0.0)						
206	Thr	105.2 (0.0)	176.4 (0.7)	62.1 (0.0)	72.7 (0.2)			21.3 (- 0.3)		
207	Gly	111.9 (- 0.3)	171.8 (0.4)	45.7 (0.2)						
224	Asn	119.7 (- 0.4)		55.1 (0.1)	36.3 (- 0.2)	174.0 (0.4)				
226	Ala		180.0 (0.0)		18.7 (0.3)					
227	Asp	118.5 (- 0.5)	180.8 (0.0)	58.3 (0.0)	40.4 (0.0)	178.6 (-0.2)				
230	Asn	114.0 (- 0.1)		55.0 (0.0)		171.4 (0.2)				
232	Ile			67.4 (- 0.1)	37.2 (0.1)		29.0 (0.2)	16.3 (0.1)		13.8 (0.1)
235	Gly		176.8 (0.4)	47.7 (0.1)						
238	Ile	122.2 (- 0.2)		65.2 (0.1)	37.7 (0.3)		29.6 (0.1)	17.2 (0.1)		14.7 (- 0.1)
240	Asn	114.1 (- 0.3)	176.6 (- 0.1)	57.1 (0.0)	39.8 (- 0.3)					
242	Ala	126.1 (- 0.1)	181.0 (0.4)	54.4 (0.1)	20.0 (0.3)					

Data analysis. An example input file for SIMPSON [8] simulations of HLF-HCCH modulation curves. The spin system parameters are given as example only.

```
spinsys {
 channels 13C 1H
 nuclei   13C 13C 1H 1H

# Retinal H-C14-C15-H in trans conformation
# change this part while using for other systems/conformations
   dipole 1 2 -2710.55 0 90 0
   dipole 1 3 -11945.49 0 90 -114.98
   dipole 1 4 -1740.153 0 90 28.487
   dipole 2 3 -1740.153 0 90 -151.51
   dipole 2 4 -11945.49 0 90 65.023
   dipole 3 4 -3925.7 0 90 40.903
}

par {
   proton_frequency 393e6
   spin_rate        8000
   crystal_file     rep256
   gamma_angles     20
   np               64
   start_operator   I1z+I2z
   detect_operator  I1z+I2z
   verbose          1111
   sw               0.5*spin_rate*(np-1)
}

proc pulseq {} {
   global par
# parameters needed for POST-C7
   set rperiod [expr 1.0e6/$par(spin_rate)]
   set rf [expr 7.0*$par(spin_rate)]
   set t90 [expr 0.25e6/$rf]
# calculation of step size during t1
   set step [expr (1.0*$rperiod / ($par(np)-1) )]
   maxdt $step
# DQ-filter
   matrix set 2 totalcoherence {2 -2}
   reset 0

# define propagators for DQ excitation and reconversion
# define POST-C7 DQ exication
   for {set i 1} {$i <= 7} {incr i} {
      set phase [expr $i*360.0/7.0]
      turnoff dipole_1_3 dipole_2_4 dipole_1_4 dipole_2_3 dipole_3_4
      pulse $t90 $rf $phase 0 0
      pulse [expr 4.0*$t90] $rf [expr $phase+180] 0 0
      pulse [expr 3.0*$t90] $rf $phase 0 0
   }
   store 1
   reset

# define POST-C-7 DQ reconversion
   for {set i 1} {$i <= 7} {incr i} {
      set phase [expr 90-$i*360.0/7.0]
      turnoff dipole_1_3 dipole_2_4 dipole_1_4 dipole_2_3 dipole_3_4
      pulse [expr 3.0*$t90] $rf $phase 0 0
      pulse [expr 4.0*$t90] $rf [expr $phase+180] 0 0
      pulse $t90 $rf $phase 0 0
   }
   store 2
   reset

   for {set j 0} {$j < $par(np)} {incr j} {
      set t1 [expr ((1.0*$rperiod) * $j / ($par(np)-1)) ]
      reset
# DQ excitation
      prop 1
      prop 1
      filter 2


# cw - fslg - pi - fslg - cw
# -----t_r----pi----t_r-----
```

```
      turnoff dipole_1_3 dipole_2_4 dipole_1_4 dipole_2_3  dipole_3_4
      delay [expr (1.0*$rperiod - $t1)]
      turnon dipole_1_3 dipole_2_4 dipole_1_4 dipole_2_3
      delay $t1
      pulseid 2 250000 x 0 0
      delay $t1
      turnoff dipole_1_3 dipole_2_4 dipole_1_4 dipole_2_3 dipole_3_4
      delay [expr (1.0*$rperiod - $t1)]

# DQ reconversion
      turnon all
      prop 2
      prop 2
      acq
   }
}

proc main {} {
   global par
   set f [fsimpson]
   faddlb $f 0 0
   fsave $f HCCH.dat -xreim
   funload $f
}
```

References

(1) Yao, X. L.; Schmidt-Rohr, K.; Hong, M. *J. Magn. Reson.* **2001**, *149*, 139.

(2) Ran, T.; Ozorowski, G.; Gao, Y.; Sineshchekov, O. A.; Wang, W.; Spudich, J. L.; Luecke, H. *Acta Crystallogr D* **2013**, *69*, 1965.

(3) Lai, W. C.; McLean, N.; Gansmuller, A.; Verhoeven, M. A.; Antonioli, G. C.; Carravetta, M.; Duma, L.; Bovee-Geurts, P. H. M.; Johannessen, O. G.; de Groot, H. J. M.; Lugtenburg, J.; Emsley, L.; Brown, S. P.; Brown, R. C. D.; DeGrip, W. J.; Levitt, M. H. *J. Am. Chem. Soc.* **2006**, *128*, 3878.

(4) Duma, L.; Lai, W. C.; Carravetta, M.; Emsley, L.; Brown, S. P.; Levitt, M. H. *Chemphyschem* **2004**, *5*, 815.

(5) Wittig, I.; Braun, H.-P.; Schaegger, H. *Nature Protocols* **2006**, *1*, 418.

(6) Hoffmann, J.; Aslimovska, L.; Bamann, C.; Glaubitz, C.; Bamberg, E.; Brutschy, B. *Phys. Chem. Chem. Phys.* **2010**, *12*, 3480.

(7) Klyszejko, A. L.; Shastri, S.; Mari, S. A.; Grubmuller, H.; Muller, D. J.; Glaubitz, C. *J. Mol. Biol.* **2008**, *376*, 35.

(8) Bak, M.; Rasmussen, J. T.; Nielsen, N. C. *J. Magn. Reson.* **2011**, *213*, 366.